Synthesis of mesoporous zeolite catalysts by in situ formation of carbon template over nickel nanoparticles

Abildstrøm, Jacob Oskar; Kegnæs, Marina; Hytoft, Glen; Mielby, Jerrik Jørgen; Kegnæs, Søren

Published in:
Microporous and Mesoporous Materials

Link to article, DOI:
10.1016/j.micromeso.2015.12.015

Publication date:
2016

Document Version
Peer reviewed version

Synthesis of mesoporous zeolite catalysts by *in situ* formation of carbon template over nickel nanoparticles

Jacob Oskar Abildstrøm[a], Marina Kegnæs[b], Glen Hytoft[b], Jerrik Mielby[a], Søren Kegnæs[a,*]

[a]*Department of Chemistry, Technical University of Denmark, DK-2800 Kgs. Lyngby, Denmark*

[b]*Haldor Topsøe A/S, Haldor Topsøes Allé 1, DK-2800 Kgs. Lyngby, Denmark*

* Corresponding author.

E-mail: skk@kemi.dtu.dk

Abstract

A novel synthesis procedure for the preparation of the hierarchical zeolite materials with MFI structure based on the carbon templating method with *in situ* generated carbon template is presented in this study. Through chemical vapour deposition of coke on nickel nanoparticles supported on silica oxide, a carbon-silica composite is obtained and exploited as a combined carbon template/silica source for zeolite synthesis. This approach has several advantages in comparison with conventional carbon templating methods, where relatively complicated preparative strategies involving multistep impregnation procedures and rather expensive chemicals are used. Removal of the carbon template by combustion results in zeolite single crystals with intracrystalline pore volumes between 0.28 and 0.48 cm^3/g. The prepared zeolites are characterized by XRD, SEM, TEM and physisorption analysis. The isomerization and cracking of *n*–octane is chosen as a model test reaction and the mesoporous zeolite catalyst is found to exhibit higher activity than the conventional catalyst.

Keywords:

Hierarchical zeolites, carbon templating, metal nanoparticles, cracking, isomerization.

1. Introduction

Zeolites represent the most important group of industrial catalysts offering a wide range of applications from oil refining, petrochemistry and the synthesis of fine chemicals to environmental catalysis [1-4]. Zeolites are crystalline microporous materials that possess a well-defined structure with pore sizes in the range of molecular dimensions as well as strong acid sites. This makes zeolites unique catalysts that can provide excellent size– and shape-selectivity. Moreover, their tuneable chemical composition, high surface area and large pore volume along with high thermal, hydrothermal and mechanical stability make zeolites very attractive heterogeneous catalysts [5, 6] and support materials that can incorporate metal nanoparticles or nanoclusters inside the micropore cavities [7-9]. Furthermore, zeolites modified with metal nanoparticles may combine the attractive properties of zeolites with the special catalytic properties of metal nanoparticles to give novel bifunctional catalytic materials where synergistic effects are exploited [10-12].

Unfortunately, zeolites often suffer from severe diffusion limitations that in some cases may induce a negative impact on the catalytic performance of zeolite catalysts. This is related to the intracrystalline transport of the reactants and products to and from the active sites in the zeolites, especially in the reactions that involve large and bulky compounds. Additionally, in some reactions, coke formation enhances these limitations, as the coke deposits block the zeolite micropores, causing a rapid decrease in the

catalytic activity [13, 14]. Therefore, large efforts have been made in order to improve the catalyst performance. This has been realized by reduction of the intracrystalline diffusion path length in the following possible approaches: synthesis of zeolites with extra-large pores [15-20], direct synthesis of zeolite nanocrystals [21-27], by exfoliating layered zeolites [28, 29], and by introducing mesopores in the microporous materials through templating strategies [14, 30, 31] or demetallation processes [4, 32-36].

Over the last years hard-templating strategies for the preparation of hierarchical zeolites and particularly the carbon templating method for the preparation of mesoporous materials have attracted considerable attention [14, 30, 37, 38]. The creation of mesoporosity is beneficial for catalytic applications as it facilitates efficient mass transport of reactants and products in the mesopores [33]. Additionally, mesoporosity in zeolites leads to a better dispersion of active metal particles to maximize the catalyst performance [12]. Recently the benefits of introducing mesopores into zeolite crystals by carbon templating have been demonstrated [39-43]. The mesoporous zeolite crystals combine the shape-selectivity, hydrothermal stability and high acidity typical for conventional zeolites with highly efficient transport of reactants and products typical for mesoporous materials. However, in spite of numerous advantages, the carbon templating method has never been implemented industrially, due to several practical challenges including versatility in terms of zeolite structure and compositions, feasibility of tailoring the hierarchical features and ease of being scaled up in a cost-effective way [30].

Here we report the recent progress on synthesis of mesoporous zeolite catalysts modified with nickel nanoparticles using a simple and versatile procedure by *in situ* formation of the carbon template. This novel approach has several advantages in

comparison with existing carbon templating methods, where relatively complicated preparative strategies involving multistep impregnation procedures are used. Furthermore, the conventional carbon templating approach often relies on relatively expensive starting materials such as carbon black pearls and tetraethylorthosilicate [14]. In the presented approach a cheap and available silica source - silica gel (SiO_2) is used. Moreover, the carbon template is generated *in situ* by decomposition of methane, which results in the formation of large amounts of coke around the silica supported nickel nanoparticles. The formation of coke over metal nanoparticles is a well-known phenomenon for a range of catalytic reactions that is frequently investigated [44]. In the presented method, the formation of coke is used to serve as carbon template during the subsequent zeolite synthesis. This approach is based on the assumption that the encapsulated carbon is removed by combustion after the zeolite crystallization, thereby creating additional porosity in the zeolite crystals. In Figure 1 a schematic overview of the presented synthesis approach is given.

By subjecting the metal nanoparticles to a varied amount of methane, the ratio of coke to silica can be tuned. In principal, this may be used to control the porosity in the mesoporous zeolites in a very simple manner. Furthermore, this synthesis method allows adjusting the acidity of the zeolites, i.e. the Si/Al ratio independently of the mesoporosity. Finally, an important advantage of this approach is the relatively versatile synthesis method that in principle allows any desired zeolite with incorporated metal nanoparticles to be prepared in mesoporous form.

In order to compare the conventional and hierarchical zeolite catalysts the cracking and isomerization of the *n*-octane is chosen as a test reaction.

2. Experimental

2.1. X-ray Powder Diffraction

X-ray powder diffraction patterns were recorded in transmission mode using Cu - Kα radiation from a focusing quartz monochromator and a Huber G760 Guinier camera in the 2θ interval 5-80°.

2.2. Nitrogen Physisorption

Nitrogen adsorption and desorption measurements were performed at liquid nitrogen temperature on a Micromeritics ASAP 2020. The samples were outgassed in vacuum at 200°C during 18 h prior to measurement. Total surface area was calculated according to the BET method. Micropore volumes (V_{micro}) were determined using *t*-plot method. The total sorbed volume (V_{total}), including adsorption in the micropores and mesopores and on the external surface, were calculated from the amount of nitrogen adsorbed at relative pressure $p/p_0 = 0.99$, before the onset of interparticle consideration. Pore size distributions were calculated by the BJH method (desorption).

2.3. Inductively Coupled Plasma

Elemental analysis was performed by ion coupled plasma optical emission spectroscopy (ICP-EOS) on a Agilent 720 ES ICP-OES instrument. Before analysis the solid samples were dissolved in a solution of H_3PO_4, HCl, and HF.

2.4. Scanning Electron Microscopy

Scanning electron microscopy (SEM) was performed on Quanta 200 ESEM FEG operated at 10 kV, with the calcined zeolite samples placed on a carbon film and Au was evaporated onto the samples for 5 seconds to achieve the sufficient conductivity.

2.5. Transmission Electron Microscopy

Transmission electron microscopy (TEM) was performed on a FEI Tecnai microscope operated at 200 kV with the samples dispersed directly on holey carbon grids.

2.6. Materials

All reagents were of reagent grade and used without further purifications: tetrapropylammonium hydroxide (TPAOH, 1M aqueous solution, Sigma-Aldrich), silica gel (SiO_2, Davisil Grade 62, pore size 150 Å, 60-200 mesh, Sigma-Aldrich), sodium aluminate ($NaAlO_2$, 54 wt % Al_2O_3 and 41 wt % Na_2O, Riedel-de Haen), ammonium nitrate (NH_4NO_3, 98 wt %, Aldrich), Nickel nitrate hexahydrate ($Ni(NO_3)_2 \cdot 6H_2O$, Sigma-Aldrich), *n*-octane (C_8H_{18}, 98%, Sigma-Aldrich), methane gas (CH_4, AGA), forming gas (10% H_2/N_2, AGA), and distilled water.

2.7.1. Preparation of Ni-containing Silica-carbon composite materials

The silica-carbon composite was prepared by the following procedure. 0.15 g of $Ni(NO_3)_2 \cdot 6H_2O$ was dissolved in 1.73 g of water. 1.50 g of SiO_2 was impregnated with this solution to incipient wetness. The resulting material was dried overnight at room temperature and then calcined in a flow of 10% H_2/N_2 (with a ramp of 20 ^oC/min) at 600 ^oC for 4 h (Sample 1) and for 8 h (Sample 5), followed by calcination in a flow of

Ar until temperature was fallen to 550 °C. One of the samples (Sample 4) was not reduced in the flow of 10% H_2/N_2. Then flow was changed to a flow of CH_4 and the obtained materials were subjected to it at 550 °C for 8 hours.

2.7.2. Synthesis of Ni-containing mesoporous ZSM-5-type zeolite

The mesoporous Ni-containing Na-ZSM-5 material was prepared according to the following procedure. In a 100 ml flask, 8.73 g of TPAOH, 0.60 g of H_2O, and 0.06 g of $NaAlO_2$ was added with stirring until a clear solution was obtained. After that, the Ni-containing silica-carbon composite obtained above (2.6.1) was mixed with this solution. The composition of the resulting synthesis gel was 1 Al_2O_3 : 78 SiO_2 : 13TPA_2O : 1.4 Na_2O : 1313 H_2O. After 1 h in case of Sample 1 and after 20 h in case of Sample 3, the final composite material was placed in a teflon beaker inside a stainless steel autoclave, containing 15 ml of water to produce saturated steam, heated to 180 °C and kept there for 72 h. Then, the autoclave was cooled to room temperature, the product was washed with deionized water (1 l) and filtered by suction. Finally, the product was dried at 90 °C for 10 h, and the organic template and the carbon was removed by controlled combustion in air in a muffle furnace at 550 °C for 24 h. Finally, the product was calcined in a flow of 10% H_2/N_2 (with a ramp of 20 degree/min) at 600 °C for 4 h.

2.7.3. Synthesis of Ni-containing conventional ZSM-5-type zeolite

The conventional Ni-containing Na-ZSM-5 material (Sample 2) was prepared according to the following procedure. 0.15 g of $Ni(NO_3)_2 \cdot 6H_2O$ was dissolved in 1.73 g of water. 1.50 g of SiO_2 was impregnated with this solution to incipient wetness. The resulting material was dried overnight at room temperature. In a 100 ml flask, 8.73 g of

TPAOH, 0.60 g of H_2O, and 0.06 g of $NaAlO_2$ was added with stirring until a clear solution was obtained. After that, the Ni-containing silica oxide was mixed with this solution. The composition of the resulting synthesis gel was 1 Al_2O_3 : 78 SiO_2 : 13TPA_2O : 1.4 Na_2O : 1313 H_2O. After 1 h, the final composite material was placed in a teflon beaker inside a stainless steel autoclave, containing 15 ml of water to produce saturated steam, heated to 180 ^oC and kept there for 72 h. Then, the autoclave was cooled to room temperature, the product was washed with deionized water (1 l) and filtered by suction. The zeolite was dried at 90 ^oC for 10 h, and the organic template and the carbon was removed by controlled combustion in air in a muffle furnace at 550 ^oC for 24 h. Finally, the product was calcined in a flow of 10% H_2/N_2 (with a ramp of 20 ^oC/min) at 600 ^oC for 4 h.

2.8. Catalysts preparation

2.8.1. Ion Exchange

All acidic zeolite samples (Ni-H-ZSM-5) were prepared by the following ion-exchange procedure. The H-form of each zeolite was prepared by three consecutive ion-exchanges, starting with the corresponding Na-form (1 g of sample) and 1 M aqueous NH_4NO_3 solution (80 ml) at 80 ^oC. The filtered NH_4-form of zeolite was washed with deionized water (1 l) after each exchange and allowed to dry in air. Finally, the ion-exchanged product was heated in air at 550 ^oC for 5 h to produce the desired H-form of the zeolite.

2.9. Catalytic Experiments: cracking and isomerization of n-octane

In the *n*-octane conversion experiments, 100 mg of fractionated catalyst (180 – 355 µm) was placed into a 3 mm stainless steel fixed-bed reactor. Afterwards, *n*-octane was pumped into an evaporator at 180 °C together with H_2 (50 ml/min) and the preheated gas was then passed through the reactor. All activity measurements were performed under the same reaction conditions using a pre-programmed temperature profile from 300 - 500 °C increasing with 1 °C/min.

The product gas was periodically analysed every 20 min by an online GC-FID equipped with a standard nonpolar column. All major products were identified from gas samples by GC-MS and by the retention time of authentic samples on the online GC-FID.

3. Results and discussion

X-ray powder diffraction patterns for all produced MFI-type zeolites after the zeolite synthesis and subsequent combustion of the organic template and the carbon material are shown in Figure 2. Based on these data, all obtained zeolites are concluded to be completely crystalline and contain exclusively MFI-structured material.

Figure 3 (A) shows the nitrogen adsorption/desorption isotherm of Ni-containing mesoporous zeolite after combustion of the carbon. The isotherm contains a hysteresis loop at relative pressure higher than $p/p_0 = 0.4$, which is indicative for mesoporosity. Moreover, the hysteresis loop has an upward curvature at relative pressure above 0.8. This upward curvature indicates the presence of cylindrical mesopores which are connected to the external surface area [45]. Additionally, as it is seen from Figure 3 (B) mesopores with a diameter of about 17 nm are formed. By varying process parameters

as described in 2.7.1 and in 2.7.2, the zeolite samples with different amount of mesoporosity and with pore volumes of up to 0.48 cm^3/g can be formed, as it is seen in Figure 3 (C) and Table 1 and Table 2. Nitrogen physisorption isotherms for these materials as well as XRPD patterns are presented in supplementary materials.

Table 1. Nitrogen physisorption and elemental analysis data

Sample name	Zeolite	Conv/ Meso	Si/Al ratio[a]	V_{micro} $(cm^3/g)^b$	V_{total} (cm^3/g)	Surface Area $(m^2/g)^c$	Ni content (wt%)[a]
Sample 1	Ni-HZSM-5	meso	39	0.09	0.28	429	1.9
Sample 2	Ni-HZSM-5	conv	42	0.10	0.20	388	1.7

[a]Determined by ICP; [b]Calculated by *t*-plot metod; [c]Calculated by BET method

Table 2. Nitrogen physisorption data for samples presented in Figure 3 (C).

Sample name	Zeolite	Conv/ Meso	V_{micro} $(cm^3/g)^a$	V_{total} (cm^3/g)	Surface Area $(m^2/g)^b$
Sample 3	Ni-HZSM-5	meso	0.12	0.46	432
Sample 4	Ni-HZSM-5	meso	0.11	0.48	448
Sample 5	Ni-HZSM-5	meso	0.13	0.40	433

[a]Calculated by *t*-plot method; [b]Calculated by BET method

It is apparent from Figure 3 (B) and Table 1 that mesoporous Ni-containing zeolite sample obtained by novel method using *in situ* generated carbon template has standard pores volumes and is characterized by large surface area [46]. Moreover, it is seen from Table 1 that by using the presented synthesis method it is possible easily to obtain mesoporous zeolite crystals with desirable acidity (matching the acidity of conventional materials), which is challenging in the case of conventional carbon templating method [46]. Temperature programmed desorption of ammonia (NH_3-TPD) for two samples presented in Table 1 showed very similar results, see Figure S5 in supplementary materials.

Figure 4 shows representative SEM images of the conventional and mesoporous Ni-ZSM-5 zeolites after combustion of the carbon template. The SEM images indicate that both samples are highly crystalline and that crystals of uniform size are obtained. The average crystal size of both conventional and mesoporous zeolites determined from SEM images in Figure 4 and from TEM image in Figure 5 and is about 1 μm and the typical shape of MFI-type crystals is observed.

From TEM image in Figure 5 (A), it is possible to see the individual mesopores, which are in good agreement with the pore size distribution determined by physisorption analysis. The incorporated nickel particles have an average particle size of around 6 nm as determined by TEM (Figure 5(B)).

The TEM images of conventional ZSM-5 material are available in supplementary materials.

As a test reaction for conventional and mesoporous Ni-HZSM-5 the cracking and isomerization of the long chain alkane *n*-octane is chosen. Figure 6 shows the catalyst performance in terms of conversion of *n*-octane. Clearly, there is a pronounced effect of the presence of mesopores in the catalyst, which can be attributed to the enhanced diffusion properties of the zeolite crystal compared to the conventional zeolite catalysts. This is particularly important for reactions that involve reactants more bulky than *n*-octane. The product distributions at 450 ^{o}C for the conventional and mesoporous Ni-HZSM-5 catalysts are given in supplementary materials, Figure S6 and S7. It is seen that the product distributions for two catalysts are similar. The mesoporous zeolite catalyst gave smaller fraction of C2 and a slightly larger faction of C5 and C6 in the product mixture in comparison with the conventional zeolite catalyst. Improved

catalytic selectivity for mesoporous zeolite catalysts has also been observed previously [40].

4. Conclusions

In conclusion, the preparation of mesoporous ZSM-5-type zeolite single crystals modified with Ni-nanoparticles based on the carbon templating method with *in situ* generated carbon template is reported for the first time. The obtained zeolite material combines high crystallinity with an intracrystalline mesopore system with pore volume of up to 0.4 cm^3/g. Compared to existing carbon templating procedures, this method does not rely on the availability of special and expensive chemicals, only on the mesoporous silicas that are used widely and can be obtained easily by precipitation. Thus, with this novel and simple preparation method, it will be possible that mesoporous zeolites with incorporated nickel nanoparticles could be so easily and inexpensively available that they will find use in industrial applications.

Acknowledgements

The authors thank Mette Nielsen (Haldor Topsøe A/S) for assistance during catalyst characterization. The authors gratefully acknowledge the support of the Danish Council for Independent Research, Grant No. 2-127580 and the support of the Lundbeck Foundation (Lundbeckfonden), Grant No. R141-2013-13244.

References

[1] W. Vermeiren, J.-P. Gilson, Top. Catal. 52 (2009) 1131-1161.

[2] C. Martínez, A. Corma, Coord. Chem. Rev. 255 (2011) 1558-1580.

[3] J. Cejka, G. Centi, J. Perez-Pariente, W. J. Roth, Catal. Today 179 (2012) 2-15.

[4] V. Valtchev, G. Majano, S. Mintova, J. Pérez-Ramírez, Chem. Soc. Rev.42 (2013) 263-290.

[5] R. Szostak, Molecular Sieves - Principles of Synthesis and Identification, Van Nostrand Reinhold: New York, 1989; 2nd ed.; Blackie: London (1998) 1-5.

[6] A. Corma, Chem. Rev. 95 (1995) 559-614.

[7] J. C. Fierro-Gonzalez , Y. Hao, B. C. Gates, J. Phys. Chem. C 111 (2007) 6645-6651.

[8] A. B. Laursen, K. T. Højholt, L. F. Lundegaard, S. B. Simonsen, S. Helveg, F. Schüth, M. Paul, J.-D. Grunwaldt, S. Kegnæs, C. H. Christensen, K. Egeblad, Angew. Chem. Int. Ed. 49 (2010) 3504-3507.

[9] K. T. Højholt, A. B. Laursen, S. Kegnæs, C. H. Christensen, Top. Catal. 54 (2011) 1026-1033.

[10] C. H. Christensen, B. Jørgensen, J. Rass-Hansen, K. Egeblad, R. Madsen, S. K. Klitgaard, S. M. Hansen, M. R. Hansen, H. C. Andersen, A. Riisager, Angew. Chem. Int. Ed. 45(28) (2006) 4648-4651.

[11] P. M. Arnal, M. Comotti, F. Schüth, Angew. Chem. 118 (2006) 8404-8407.

[12] J. Mielby, J. O. Abildstrøm, F. Wang, T. Kasama, C. Weidenthaler, S. Kegnæs, Angew Chem. Int. Ed. 53 (2014) 12513-12516.

[13] C. H. Christensen, K. Johannsen, E. Törnqvist, I. Schmidt, H. Topsøe, C. H. Christensen, Catal. Today 128 (2007) 117-122.

[14] K. Egeblad, C. H. Christensen, M. Kustova, C. H. Christensen, Chem. Mater. 20 (2008) 946-960.

[15] M. E. Davis, C. Saldarriaga, C. Montes, J. Garces, C. Crowder, Nature 331 (1988) 698-699.

[16] C. C. Freyhardt, M. Tsapatsis, R. F. Lobo, K. J. Balkus, Jr., M. E. Davis, Nature 381 (1996) 295-298.

[17] A. Corma, M. J. Diaz-Cabanas, J. L. Jorda, C. Martinez, M. Moliner, Nature 443 (2006) 842-845.

[18] J. Sun, C. Bonneau, A. Cantin, A. Corma, M.J. Diaz-Cabanas, M. Moliner, D. Zhang, M. Li, X. Zou, Nature 458 (2009) 1154-1158.

[19] R. Simancas, D. Dari, N. Velamazán, M.T. Navarro, A. Cantín, J.L. Jordá, G. Sastre, A. Corma, F. Rey, Science 26 (2010) 1219-1222.

[20] O. V. Shvets, P.Nachtigall, W. J. Roth, J. Cejka, Micropor. Mesopor. Mater. 182 (2013) 229-238.

[21] G. Bellussi, A. Carati, M.G. Clerici, G. Meddinelli, R. Millini, J. Catal. 133 (1992) 220-230.

[22] L. Tosheva, V. Valtchev, Chem. Mater. 17 (2005) 2494–2513.

[23] M. Choi, K. Na, J. Kim, Y. Sakamoto, O. Terasaki, R. Ryoo, Nature 461 (2009) 246–249.

[24] M. Tsapatsis, W. Fan, Chem. Cat. Chem. 2 (2010) 246–248.

[25] X. Zhang, D. Liu, D. Xu, S. Asahina, K. A. Cychosz, K. V. Agrawal, Y. A. Wahedi, A. Bhan, S. A. Hashimi, O. Terasaki, M. Thommes, M. Tsapatsis, Science 336 (2012) 1684-1687.

[26] W. Chaikittisilp, Y. Suzuki, R. R. Mukti, T. Suzuki, K.Sugita, K. Itabashi, A. Shimojima, T. Okubo, Angew Chem. 125 (2013) 3439-3443.

[27] H. Awala. J.-P. Gilson, R. Retoux, P. Boullay, J.-M. Goupil, V. Valtchev, S. Mintova, Nature Mater. 14 (2015) 447-451.

[28] A. Corma, V. Fornes, S. B. Pergher, Th. L. M. Maesen, J. G. Buglass, Nature 396 (1998) 353 – 356.

[29] S. Maheshwari, E. Jordan, S. Kumar, F. S. Bates, R. L. Penn, D. F. Shantz, M. Tsapatsis, J. Am. Chem. Soc. 130 (2008) 1507 – 1516.

[30] D. P. Serrano, J. M. Escola, P. Pizarro, Chem. Soc. Rev. 42 (2013) 4004-4035.

[31] K.Na, G. A. Somorjai, Catal. Lett. 145 (2015) 193-213.

[32] J. Perez-Ramirez, D. Verboekend, A. Bonilla, S. Abello, Adv. Funct. Mater. 19 (2009) 3972-3979.

[33] R. Chal, C. Gerardin, M. Bulut, S. van Donk, Chem. Cat. Chem. 3 (2011) 67-81.

[34] K. Na, M. Choi, R. Ryoo, Micropor. Mesopor. Mater. 166 (2013) 3-19.

[35] M. S. Holm, K. Egeblad, P. N. R. Vennestrøm, C. G. Hartmann, M. Kustova, C. H. Christensen, Eur. J. Inorg. Chem. (2008) 5185-5189.

[36] P. N. R. Vennestrøm, M. Grill, M. Kustova, K. Egeblad, L. F. Lundegaard, F. Joensen, C. H. Christensen, P. Beato, Catal. Today 168 (2011) 71-79.

[37] C. J. H. Jacobsen, C. Madsen, J. Houzvicka, I. Schmidt, A. Carlsson, J. Am. Chem. Soc. 122 (2000) 7116-7117.

[38] M. Kustova, K. Egeblad, K. Zhu, C. H. Christensen, Chem. Mater. 19 (2007) 2915-2917.

[39] M. Yu. Kustova,P. Hasselriis, C. H. Christensen, Catal. Lett. 96 (2004) 205-211.

[40] C. H. Christensen, I. Schmidt, C. H. Christensen, Catal. Commun. 5 (2004) 543-546.

[41] M. Yu. Kustova, S. B. Rasmussen, A. L. Kustov, C. H. Christensen, Appl. Catal. B 67 (2006) 60-67.

[42] M. Kustova, M. S. Holm, C. H. Christensen, Y.-H. Pan, P. Beato, T. V. W. Janssens, F. Joensen, J. Nerlov, Stud. Surf. Sci. Catal. 174 (2008) 117-122.

[43] M. S. Holm, E. Taarning, K. Egeblad, C. H. Christensen, Catal. Today 168 (2011) 3-16.

[44] A. K. Rovik, S. K. Klitgaard, S. Dahl, C. H. Christensen, I. Chorkendorff, Appl. Catal. A 358 (2009) 269-278.

[45] A. N. Janssen, I. Schmidt, C. J. H. Jacobsen, A. J. Koster, K. P. de Jong, Micropor. Mesopor. Mater. 65 (2003) 59-75.

[46] M. Yu. Kustova, A. L. Kustov, C. H. Christensen, Stud. Surf. Sci. Catal. 158 (2005) 255-262.

Figures

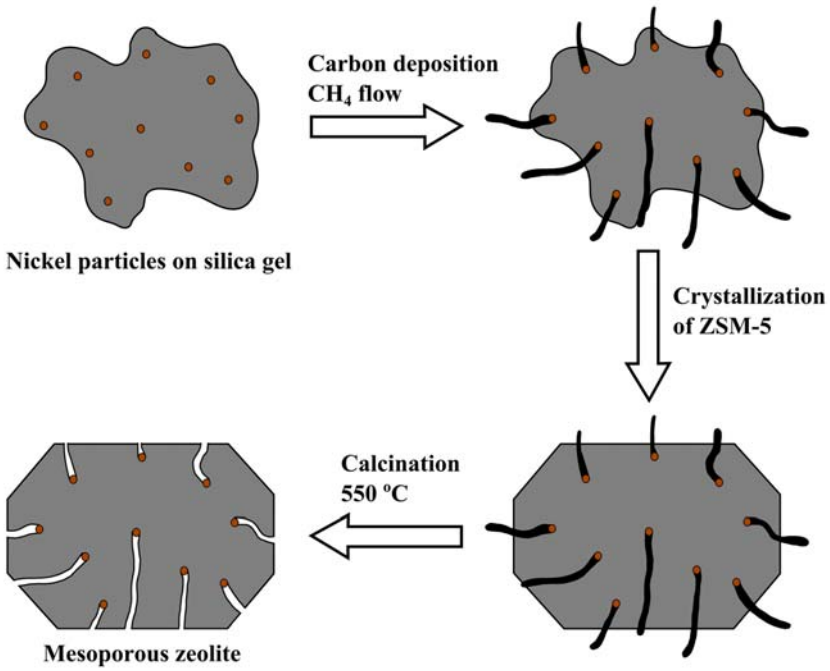

Figure 1. Overview of the synthesis process: by passing methane over nickel nanoparticles (orange), supported on silica (grey), a carbon template is generated in situ as the methane decomposes to coke (black). The obtained carbon- silica composite is then transformed into zeolite during crystallization, incorporating the nickel nanoparticles and carbon. Combustion of the carbon template results in a mesoporous zeolite containing nickel nanoparticles.

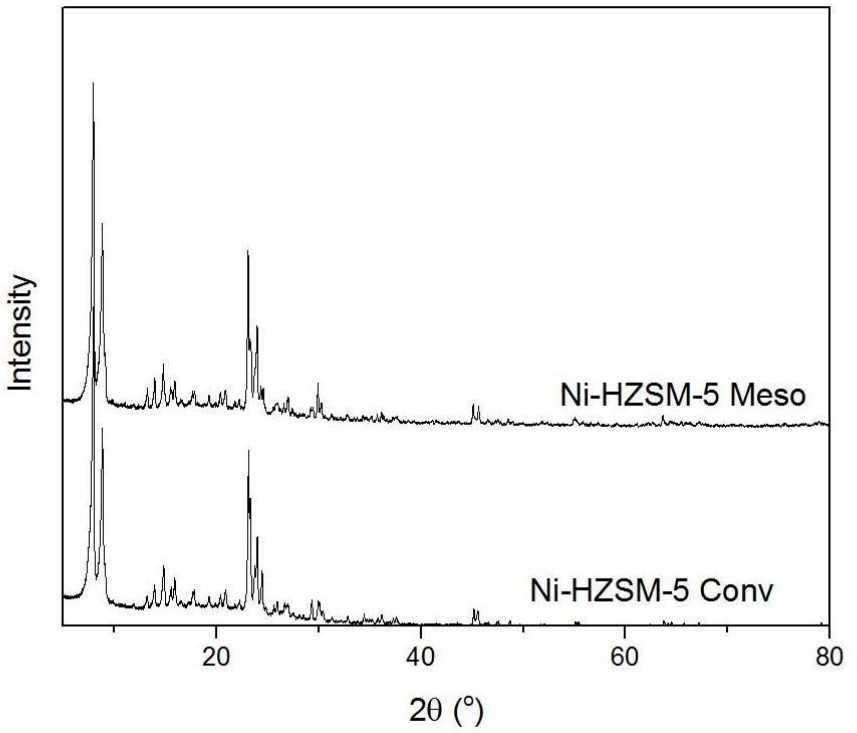

Figure 2. XPRD patterns of pure and Ni-containing conventional (sample 2) and mesoporous (sample 1) MFI-type materials.

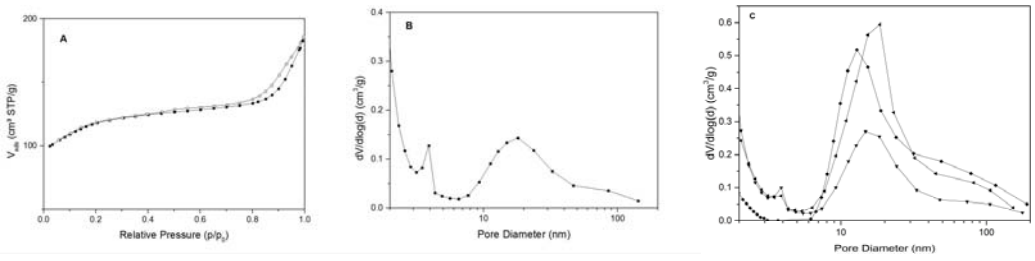

Figure 3. (A) N_2 adsorption/desorption isotherm of the mesoporous Ni-containing HZSM-5-type material and (B) BJH-derived pore-size distribution of sample 1.(C) BJH-derived pore-size distribution of sample 3 (▼), sample 4(◄) and sample 5 (♦).

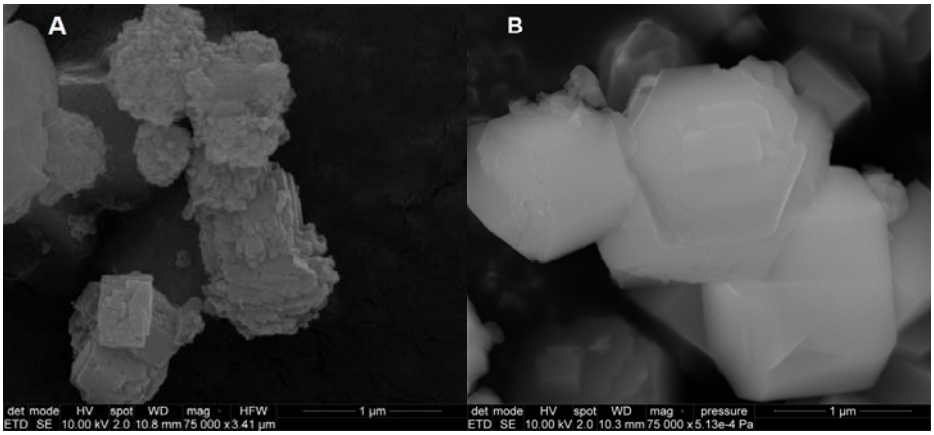

Figure 4. SEM images of (A) mesoporous Ni-containing HZSM-5 (sample 1) and (B) microporous Ni-containing HZSM-5-type materials (sample 2).

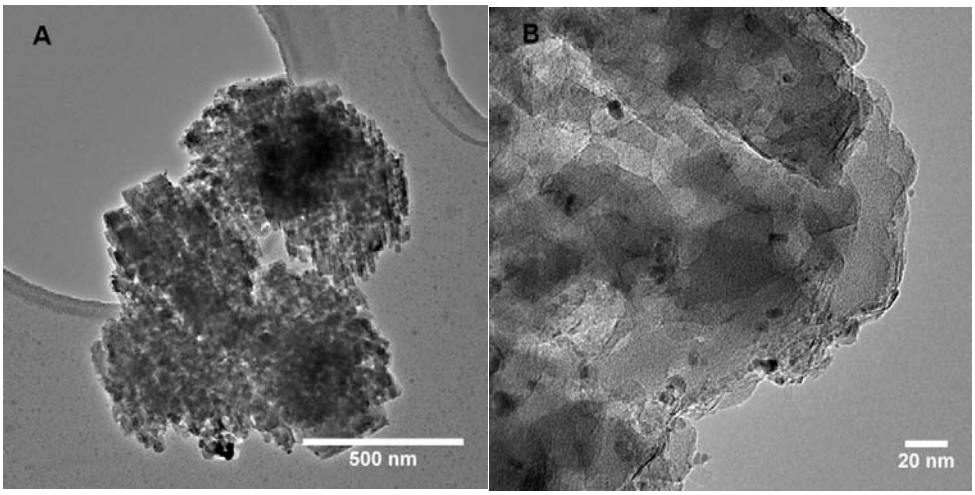

Figure 5. TEM images of mesoporous Ni-containing HZSM-5-type material (sample 1).

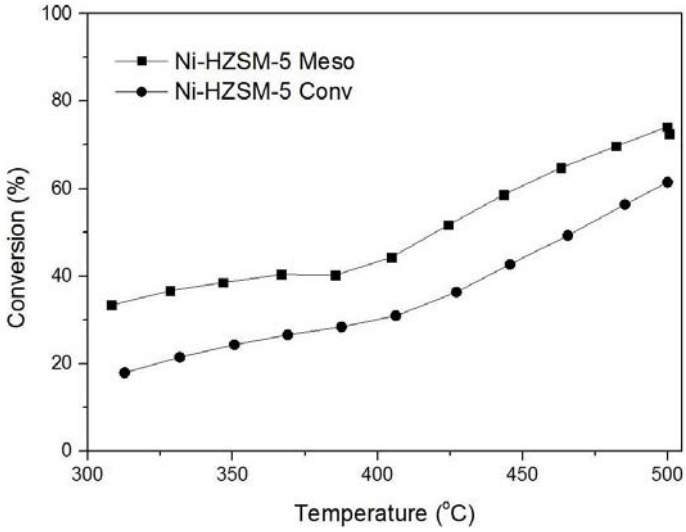

Figure 6. Conversion of n-octane over mesoporous Ni-containing HZSM-5 (sample 1) and conventional Ni-containing HZSM-5-type materials (sample 2).